Changes in Biological Activity and Folding of Guanylate Cyclase-Activating Protein 1 as a Function of Calcium†

Maria Rudnicka-Nawrot,‡ Irina Surgucheva,§ Jeffrey D. Hulmes,|| Françoise Haeseleer,‡ Izabela Sokal,‡ John W. Crabb,|| Wolfgang Baehr,§ and Krzysztof Palczewski*,‡,⊥

Departments of Ophthalmology and Pharmacology, School of Medicine, University of Washington, Seattle, Washington 98195, Moran Eye Center, University of Utah Health Science Center, Salt Lake City, Utah 84132, and W. Alton Jones Cell Science Center, Lake Placid, New York 12946

Received September 16, 1997; Revised Manuscript Received October 23, 1997⊗

ABSTRACT: Guanylate cyclase-activating protein 1 (GCAP1), a photoreceptor-specific Ca^{2+}-binding protein, activates retinal guanylate cyclase 1 (GC1) during the recovery phase of phototransduction. In contrast to other Ca^{2+}-binding proteins from the calmodulin superfamily, the Ca^{2+}-free form of GCAP1 stimulates the effector enzyme. In this study, we analyzed the Ca^{2+}-dependent changes in GCAP1 structure by limited proteolysis and mutagenesis in order to understand the mechanism of Ca^{2+}-sensitive modulation of GC1 activity. The change from a Ca^{2+}-bound to a Ca^{2+}-free form of GCAP1 increased susceptibility of Ca^{2+}-free GCAP1 to proteolysis by trypsin. Sequencing data revealed that in the Ca^{2+}-bound form, only the N-terminus (myristoylated Gly^2−Lys^9) and C-terminus (171−205 fragment) of GCAP1 are removed by trypsin, while in the Ca^{2+}-free form, GCAP1 is readily degraded to small fragments. Successive inactivation of each of the functional EF loops by site-directed mutagenesis showed that only EF3 and EF4 contribute to a Ca^{2+}-dependent inactivation of GCAP1. GCAP1($E^{75}D$,$E^{111}D$,$E^{155}D$) mutant did not bind Ca^{2+} and stimulated GC1 in a $[Ca^{2+}]$-independent manner. GCAP1 and GCAP2, but not S-100β, a high $[Ca^{2+}]_{free}$ activator of GC1, competed with the triple mutant at high $[Ca^{2+}]_{free}$, inhibiting GC1 with similar IC_{50}'s. These competition results are consistent with comparable affinities between GC1 and GCAPs. Our data suggest that GCAP1 undergoes major conformational changes during Ca^{2+} binding and that EF3 and EF4 motifs are responsible for changes in the GCAP1 structure that converts this protein from the activator to the inhibitor of GC1.

Calcium ions, Ca^{2+}, play a crucial role in cellular signaling. Because they are nondegradable, several systems have evolved to regulate the cellular concentration of free Ca^{2+} ($[Ca^{2+}]_{free}$), including intracellular compartmentalization/sequestration, pumping to the extracellular space, and buffering by Ca^{2+}-binding proteins. Some of these Ca^{2+}-binding proteins are also poised to take advantage of transient changes in $[Ca^{2+}]_{free}$ to affect properties of regulatory enzymes and ion channels. In cells that lower their internal $[Ca^{2+}]_{free}$ upon excitation, such as rod and cone photoreceptor cells, distinct types of proteins have evolved that act as activators of effector enzymes when they are in the Ca^{2+}-free state. Guanylate cyclase-activating proteins, GCAP1[1] and GCAP2, were found to fulfill such functions in the regulation of photoreceptor guanylate cyclase (GC1) (*1*−*4*).

GCAP1 and GCAP2 are acidic, ∼23-kDa, homologous proteins that contain three functional high-affinity, EF-hand Ca^{2+}-chelating motifs (reviewed in ref 5). At low $[Ca^{2+}]_{free}$, GCAPs increase the activity of GC1 (*6*) at least 10-fold (*1*) by an unknown mechanism. GCAP1 forms a stable complex with GC1, independent of $[Ca^{2+}]_{free}$. The GC1/GCAP1 complex may switch between two conformations, active and inactive, with the binding or dissociation of Ca^{2+} (*2*, *7*). GCAP2 may translocate from the cytosol to the membrane-bound cyclase when it is free of Ca^{2+} and stimulates GC1 activity (*8*). The N-terminal fatty acid-acylated regions of both GCAPs show weak sequence conservation, and the function of this region remains speculative. It is possible that the N-terminus is flexible and exposed, providing hydrophobic tethering to the membranes for the most efficient stimulation of GC1, as proposed for GCAP1 by Otto-Bruc *et al.* (*9*), but this modification is functionally unrelated in the GC1 stimulation by GCAP2, as proposed by Olshevskaya *et al.* (*8*).

† This research was supported by grants from NIH EY08061, EY06603, EY08123; Core Facilities Grants EY01730 and an award from Research to Prevent Blindness, Inc. (RPB), to the Department of Ophthalmology at the University of Washington, and the University of Utah. KP is a recipient of a Jules and Doris Stein Professorship from RPB.

* Address correspondence to this author at the University of Washington, Department of Ophthalmology, Box 356485, Seattle, WA 98195-6485. Phone: 206-543-9074. Fax: 206-543-4414.

‡ Department of Ophthalmology.

§ University of Utah Health Science Center.

|| W. Alton Jones Cell Science Center.

⊥ Department of Pharmacology.

⊗ Abstract published in *Advance ACS Abstracts,* December 1, 1997.

[1] Abbreviations: BTP, 1,3-bis[[tris(hydroxymethyl)methyl]amino]-propane; GC1, photoreceptor guanylate cyclase 1; GCAP, guanylate cyclase-activating protein; ROS, rod outer segments.

S0006-2960(97)02306-4 CCC: $15.00
Published on Web 01/06/1998

Following light excitation, the stimulation of GC1 by GCAP(s) is an essential step in the recovery of photoreceptor cells to preillumination conditions (*10*). Null mutations of GC1 result in the elimination of the internal transmitter of phototransduction, cGMP (*11*−*13*). A salient feature of those findings is that GC2, the second photoreceptor cyclase (*14*), does not substitute for GC1 in cGMP production. Thus, the function, localization, and properties of GC2 in phototransduction remain to be elucidated. The stimulation of the photoreceptor type of GC (particulate GC) by intracellular proteins provides a novel mechanism to regulate these enzymes, in addition to the regulation of non-photoreceptor cyclase via extracellularly circulating peptides (reviewed in ref 15). GC1's "extracellular domain" is sequestered inside the disk membranes of rod outer segments (*16*), and its function is currently unknown. Apart from GCAP1 and GCAP2, a third GC1 activator, S-100β, was recently identified (*17*). S-100β stimulates GC1 at micromolar $[Ca^{2+}]_{free}$; however, its physiological significance and the mechanisms of GC1 stimulation are unknown.

In these studies, we provide additional evidence that GCAP1 remains in a complex with GC1 irrespective of its Ca^{2+} occupancy, that N-terminal myristoylated GCAP1 inhibits basal GC1 activity in the Ca^{2+}-bound form, that GCAP1 undergoes significant conformational changes due to Ca^{2+} binding as analyzed by limited proteolysis, that inactivation of EF-hand motifs by site-specific mutagenesis leads to constitutive activity of GCAP1 mutant in the physiological range of $[Ca^{2+}]_{free}$, and that GCAP1 and GCAP2 interaction sites on GC1 are likely to at least partially overlap, while S-100β protein interacts and activates the cyclase at a different site. Interestingly, from the structural point of view, the proteolysis data of GCAP1 resemble those obtained previously for recoverin (*31*). The effects of inactivating mutations in EF-hands of GCAP1 are similar but not identical to those reported independently for GCAP2 (*29*).

MATERIALS AND METHODS

Protein Determinations, SDS−*PAGE, and Reagents.* Concentrations of GCAP1 and its mutants were determined spectrophotometrically assuming that $A_{280nm} = 1$ was equivalent to 0.386 ± 0.056 mg/mL of the protein (1 mg/mL GCAP1 yielded $A_{280nm} = 2.58$) and that the molecular mass was 23.5 kDa (*9*). The concentrations of other proteins were determined by the method of Bradford (*18*). SDS−PAGE (*19*) and the electrotransfer of proteins onto Immobilon was carried out using a Hoefer minigel system. Ca^{2+}-binding protein S-100β was purchased from Calbiochem (cat. no. 559290), and all other reagents were obtained from Sigma.

Expression of GCAP1 in Schizosaccharomyces pombe. The GCAP1 coding sequence was amplified by PCR with primers which inserted a *Nde*I restriction site on the ATG and a 6 histidine tag just before the stop codon and cloned into pCR 2.1 vector (Invitrogen). This cDNA, after being transferred as a *Eco*RI-*Eco*RI fragment in the *Eco*RI site of pBluescript II KS+, was isolated as a *Nde*I-*Bam*HI fragment and inserted between the sites *Nde*I and *Bam*HI of the pREP1 (Leu^+) vector (*20*). pREP1 vector was obtained from Dr. K. Maundrell (Glaxo Institute, Geneva, Switzerland). The *Schizosaccharomyces pombe* (*leu1-32, h*−) strain, provided by Dr. Paul Nurse (Imperial Cancer Research Fund, London, U.K.), was grown in Edinburgh minimal medium (EMM) containing 50 μg/mL leucine and transformed with the recombinant plasmid using the LiAc procedure (*21*) except that the lithium acetate buffer was at pH 7.5 instead of 4.9. Recombinant *S. pombe* were selected on minimal medium and grown in EMM.

GCAP1-His$_6$ Purification. Recombinant *S. pombe* (5×10^{10}) were harvested by centrifugation for 5 min at 4000*g*, washed in distilled water, and resuspended in 5 mL of 10 mM Hepes, pH 7.5, containing 300 mM NaCl and 2 mM benzamidine. Yeast cells were broken by vortexing for 4 min (30 s on/off cycle on ice) with 10 mL of acid-washed glass beads (0.5-mm diameter). After centrifugation for 10 min at 35 000 rpm, the supernatant was incubated for 90 min at 4 °C with 1 mL of Ni-NTA resin. The resin was washed with the same buffer until absorption at 280 nm was <0.02, then washed with 50 mM phosphate buffer, 300 mM NaCl, 10% glycerol, pH 6.0, until the $A_{280nm} < 0.02$ and eluted with 10 mM Hepes, pH 7.5, containing 100 mM NaCl and 250 mM imidazole. Purified proteins were dialyzed against 2.5 mM Hepes, pH 7.5, containing 50 mM NaCl overnight at 4 °C.

Site-Directed Mutagenesis. To generate point mutations in the EF2, EF3, and EF4-loops of bovine GCAP1, the following sense primers were used: the $E^{75}D$ mutagenic primer was 5′-GAT TTC ATG GAC TAC GTG GCG-3′, the $E^{111}D$ mutagenic primer was 5′-GGC AAC GGA TGC ATC GAC CGC GAC GAC CTG CTC ACC-3′, and the $E^{155}D$ mutagenic primer was 5′-ATT GAC GTC AAT GGG GAT GGG GAA CTC TCC CTA GAG GAC TTC-3′. An antisense primer W233 (*22*) was used. The template for PCR was bGCAP1 in pBluescript (GCAP-19). The PCR products were purified and digested with *Nsi*I/*Sfi*I for the EF3-hand motif mutant or *Aat*II/*Sfi*I for the EF4-hand motif mutant. The fragments were cloned into pVL941gcap1 transfer vector from which the corresponding wild-type fragments had been removed. To generate double mutants, plasmids carrying a single mutation were used as a template and the desired point mutations were introduced. For triple mutants, plasmids carrying double mutations (for example, $E^{75}D$,$E^{155}D$) were used. In some cases, PCR fragments were cloned in pBluescript II vector first and then recloned using another restriction enzyme in baculovirus vector.

To create EF1-hand motif (EF1-fix), a 72-mer sense primer containing 13 substitutions was synthesized (substitutions are followed by asterisks): 5′-AGC ACC GAG TGC CAC CAG TGG TAC AAG AAG TTC G*TG G*A*T* A*AG G*A*C G*G*C G*A*C GGC CAG CTC ACC CTC G*A A* GAG. For amplification of the mutant fragment, the protocol of asymetric PCR was used (*23*). The starting concentration of 72-mer mutagenic primer was 1 μg/tube. After the first 5 cycles (96 °C for 1 min, 72 °C for 3 min), 100 ng of antisense primer (W233) was added. The amplification was continued for 25 cycles (96 °C for 1 min, 55 °C for 1 min, 72 °C for 2min). The resulting 630-bp fragment was purified, digested with *Dra*III/*Nhe*I, and cloned into pVL941gcap1 transfer vector as described above. The construct with restored EF1-hand motif and disabled EF2−4 loops of Ca^{2+}-binding sites was cloned using EF1-fix as a template and the mutagenic primers described above. All mutant DNA constructs were purified by CsCl centrifugation, and both strands of the final product were sequenced with tagged pvl941 primers flanking the insertion site. Sequencing was performed using a Licor L4000 automatic sequencer as described previously (*24*).

Expression of Bovine GC1, GCAP1, and GCAP1 Mutants in High-Five Insect Cells. Bovine GC1 (obtained from Dr. R. Sharma), bovine GCAP1, GCAP1-G2A , Δ10-GCAP1 (*9*), and other mutants were cloned into the pVL941 vector (Invitrogen), and the recombinant proteins were expressed in insect cells as described previously (*2*). GCAP1 and all mutants were immunoaffinity-purified to apparent homogeneity (*9*, *25*) and their properties studied from at least four independent preparations. In addition, the DNA sequences of all mutants were verified in the infectious virus.

Expression of Δ7-GCAP2 and Purification of Native Bovine GCAP2. The GCAP2-7 plasmid encompassing the coding sequence for GCAP2, except for the first seven amino acids, was selected in *Escherichia coli* JM109 and then transferred into *E. coli* M15. Δ7-GCAP2 tagged with His residues at the N-terminus to facilitate purification of the recombinant protein was purified as described by Otto-Bruc *et al.* (*9*). Native GCAP2 was purified from bovine retinas using immuno-affinity chromatography (*25*).

Limited Proteolysis of GCAP1 and Its Mutants. GCAP1, or its mutants (0.4 mg/mL), in 10 mM Hepes, pH 7.5, containing 100 mM NaCl, 0.1 mM $CaCl_2$ (or 0.1 mM EGTA), and 1 mM DTT was incubated with appropriate amounts of trypsin (a GCAP1-to-trypsin ratio between 55:1 and 73:1) at 37 °C. A portion of the sample was withdrawn at various times, and proteolysis was quenched by mixing the sample with a solution of N^{α}-tosyl-Lys chloromethyl ketone (0.1 mM final concentration) or phenylmethanesulfonyl fluoride and benzamidine (1 mM each). The products of digestion were analyzed by SDS−PAGE.

Electrospray Mass Spectrometry. Electrospray mass spectrometry (ESMS) and liquid chromatography ESMS (LC ESMS) were performed with a Perkin-Elmer Sciex API300 triple quadrupole mass spectrometer (Concord, Thornhill, Ontario, Canada) fitted with an articulated ion spray plenum and an atmospheric pressure ionization source (*26*). Initial tuning and calibration was performed with a standard mixture of poly(propylene glycol) (PPG) from PE Sciex. Resolution was adjusted to approximately a 50% valley between adjacent isotope peaks in a singly charged cluster, allowing singly charged ions to be identified by apparent spacing between peaks and doubly charged ions to be distinguished from those with higher charge states. Nitrogen was used as the nebulization gas (at 40 psi) and curtain gas and was supplied from a dewar (XL-45; Taylor Wharton) of liquid nitrogen (Merriam-Graves, Claremont, NH).

LC ESMS were acquired in positive ion mode at an orifice potential of 55 V over the scan range *m/z* 400−2500 using 0.25-amu steps and a total scan time of 6 s. Synthetic peptides of known mass were used to verify correct calibration during LC ESMS. The HPLC eluant was split with 20% going to the mass spectrometer and the remainder collected in 1-min fractions. Reverse-phase HPLC for LC ESMS was performed at a flow rate of 50 μL/min on a 5-μm Vydac C18 microbore column (1 × 250 mm) using an Applied Biosystems model 120A HPLC system equipped with a 75-μL dynamic mixer and aqueous acetonitrile/trifluoroacetic acid solvents. Specifically, native GCAP (15−20 μg) was digested with trypsin [for 20 min, at room temperature, 1% trypsin by weight in 10 mM Hepes, pH 7.5, containing 100 mM NaCl, 0.1 mM $CaCl_2$ (or 0.1 mM EGTA)] and 1 mM DTT (-/+EDTA). The reaction was stopped by acidification, vacuum-dried, and resuspended in 8 M urea, and 80% of total was injected onto a 5-μm Vydac HPLC C18 column (1 × 250 mm) at 0% B. Chromatography was at a flow rate of 50 μL/min with the following gradient: time 3 min, 0% B; time 43 min, 100% B. Solvent A was 0.040% trifluoroacetic acid in H_2O, and solvent B was 84% acetonitrile containing 0.036% trifluoroacetic acid.

Preparation of ROS. ROS were prepared from fresh bovine retinas (Schenk Packing Co., Inc., Stanwood, WA) according to Papermaster (*27*). ROS were suspended in 50 mM Hepes, pH 7.8, containing 60 mM KCl and 20 mM NaCl (final concentration of 8−12 mg/mL rhodopsin). Washed ROS were prepared from ROS by removing soluble proteins, including GCAP1, as described previously (*1*).

GC Assays. The GC assays were performed using [α-^{32}P]-GTP and washed ROS or using expressed GC1 as described previously (*9*). Although the data are shown without standard deviations, they are an average of two determinations. Similar results were obtained from at least three different sets of experiments performed in duplicate. Due to the high sensitivity of the GC system (*1*), the absolute values of one series occasionally varied from another by 10−15%, but with preservation of the ratio between activity of two different preparations (for example, mutants of GCAP1). Since only a limited number of the test samples could be performed in a single assay (maximally 24 samples), we always included a relevant control (low, high $[Ca^{2+}]_{free}$ and +/− GCAP1).

Electroblotting of Tryptic Fragments of GCAP1 on PVDF and Direct Protein Microsequencing. SDS−PAGE gels were placed in transfer buffer (10 mM BTP, pH 8.4) containing 10% methanol for 10 min. Electroblotting onto a PVDF membrane (Millipore, Bradford, MD) was performed at 90 V for 1 h at 4 °C. After completion of the transfer, the membrane was stained for 10 min with 0.1% Coomassie brilliant blue R-250 in 45% methanol and 10% acetic acid and then destained in 45% methanol and 7% acetic acid for 10−15 min. The bands (2 × 5 mm) corresponding to proteolytic fragments of GCAP1 were excised with a razor blade. Corresponding bands from 4−6 lanes (∼1 μg of protein) were loaded into a blot cartridge (Applied Biosystems), and 10 cycles of Edman degradation was performed to identify the N-terminal sequence using an Applied Biosystems model 470A protein sequencer.

RESULTS

Ca^{2+}-Dependent Inhibition of GC1 by GCAP. The Ca^{2+}-free form of GCAP1 stimulated 5-fold[2] photoreceptor GC in washed ROS and recombinant GC1 (expressed in High-Five insect cells) (Figure 1A). The low basal cyclase activity, which is unaffected by up to 2.5 μM $[Ca^{2+}]_{free}$, is inhibited 80% by the Ca^{2+}-loaded form of GCAP1 (Figure 1B). The dose dependency ($EC_{50} \sim 3$ μM) for the stimulation and inhibition of recombinant GC1 was comparable (Figure 1B). Similar inhibition, with $IC_{50} \sim 1.5$ μM, was found using washed ROS (data not shown). Because GCAP1 is purified using immunoaffinity chromatography and eluted at low pH, this apparent inhibition could be due to a partially

[2] Frequently, up to 10-fold stimulation is observed on freshly prepared GC in washed ROS and recombinant GC1 expressed in insect cells.

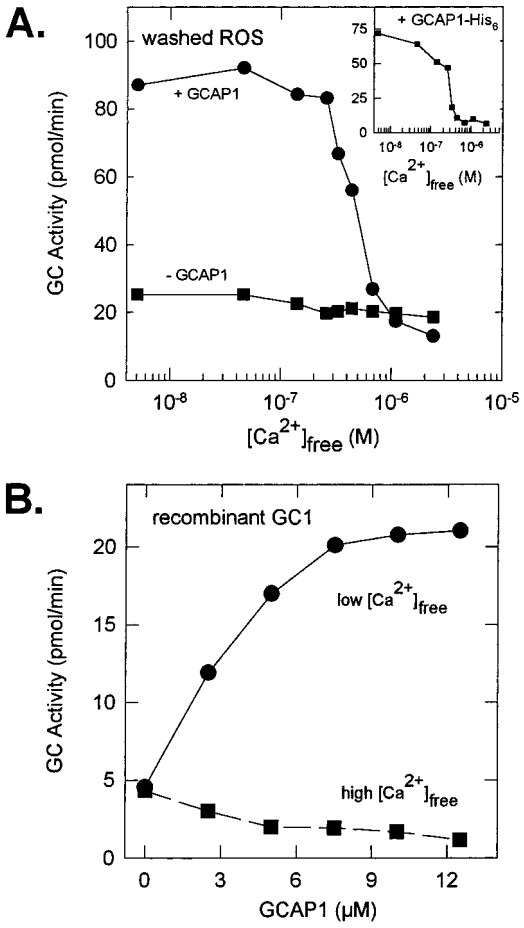

FIGURE 1: Activity of GC1 at high and low $[Ca^{2+}]_{free}$ in the presence of GCAP1. A. Ca^{2+} titration of GC activity in washed ROS. Ca^{2+} sensitivity of GC was assayed in washed ROS membranes in the presence (●) or absence (■) of 2 μM GCAP1. $[Ca^{2+}]_{free}$ was adjusted by EGTA/Ca buffer, and measurement of GC activity was carried out as described in Materials and Methods. *Inset*: GC1 in washed ROS was stimulated at different $[Ca^{2+}]_{free}$ by 2 μM GCAP1-His_6 purified in nondenaturing conditions using Ni^{2+}-chelex column. B. Stimulation of recombinant bovine GC1 expressed in High-Five insect cells by GCAP1 at low $[Ca^{2+}]_{free}$ = 10 nM and inhibition at high $[Ca^{2+}]_{free}$ = 2.5 μM.

denatured form of GCAP1. In control experiments, GCAP1-His_6, expressed in *S. pombe* yeast cells and isolated using Ni^{2+}-chelex chromatography in nondenaturating conditions, yielded myristoylated, fully active GCAP1 with properties identical to native GCAP1 or GCAP1 expressed in High-Five insect cells. These data suggest that GCAP1 stimulates at low $[Ca^{2+}]_{free}$ and inhibits GC1 at high $[Ca^{2+}]_{free}$.

Changes in GCAP1 Structure as Monitored by Limited Proteolysis. To test the effect of Ca^{2+} on the GCAP1 protein structure, limited tryptic proteolysis was performed at low and high $[Ca^{2+}]_{free}$. Large internal tryptic fragments of GCAP1 were electrotransferred on PVDF membrane and identified by Edman sequence analysis (Figure 2A). At low $[Ca^{2+}]_{free}$, N- and C-terminal (*e.g.*, cleaved at residue R^{120}) fragments of GCAP1 were rapidly produced. At high $[Ca^{2+}]_{free}$, large fragments, encompassing most of the GCAP1 sequence, were identified from PVDF electroblots (mostly cleaved at residues K^8). Concurrent with the time course of GCAP1 proteolysis, GC stimulatory activity also decreased, resulting in the inhibition of basal activity (Figure 2B). These data are consistent with inhibition of GC1 by peptides encompassing the primary sequence of GCAP1 (*9*).

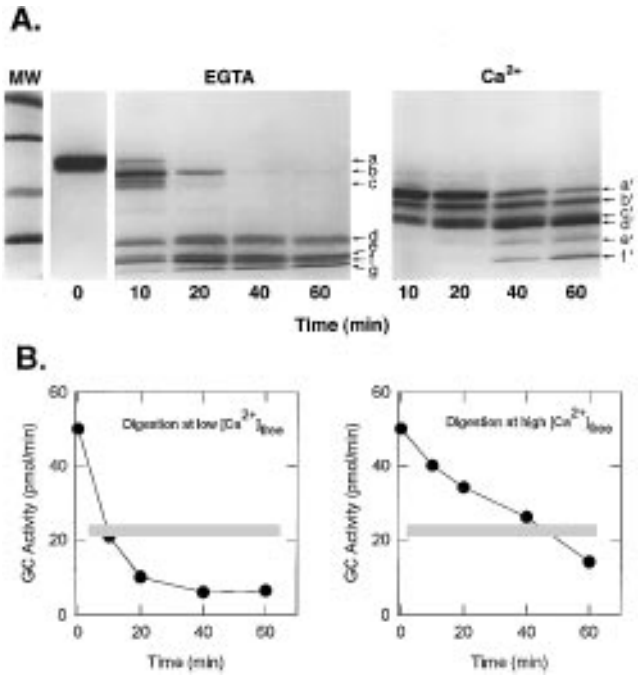

FIGURE 2: Limited proteolysis of bovine GCAP1. A. Tryptic fragments of GCAP1 were separated by SDS−PAGE as described in Materials and Methods. GCAP1 (10 μM) was digested by trypsin at a GCAP1-to-trypsin weight ratio of 60:1 (left panel) at $[Ca^{2+}]_{free}$ = 40 nM (EGTA) or (right panel) at $[Ca^{2+}]_{free}$ = 1 μM (Ca^{2+}) at 30 °C. The amino-terminal amino acids were determined by automated sequencing. The carboxyl-terminal position of the cleavage was estimated using the sequence information of peptides released from GCAP1 by trypsin and the molecular weight loss of the fragment relative to native GCAP1. The following fragment assignments were made: a, myristoylated 2−205 (native GCAP1); b, myristoylated 2−182; c, myristoylated 2−172; d, 121−205 and 121−182; e, 121−172; f, 9−91; g, dye front of the gel; a′, myristoylated 2−205; b′, myristoylated 2−196; c′, 9−182; d′, 9−178; e′, 25−172, and f′, dye front of the gel. The molecular mass markers are, from the top, 43, 30, 20, and 14 kDa. B. Decrease of GC stimulation activity by GCAP1 proteolytic fragments. GCAP1 was digested with trypsin for the indicated periods of time. Trypsin was inactivated by addition of 1 mM benzamidine and 1 mM phenylmethanesulfonyl fluoride. GC stimulation was measured as described in Materials and Methods. Horizontal shaded boxes indicate the range of the basal cyclase activity.

LC ESMS was used to identify GCAP1 peptide fragments generated by trypsin (Figure 3). The double detection method (mass spectrometry and UV absorption) allowed us to identify fragments covering essentially the complete GCAP1 polypeptide under both low and high $[Ca^{2+}]_{free}$. At low $[Ca^{2+}]_{free}$, many more tryptic fragments were generated than at high $[Ca^{2+}]_{free}$, and the masses of the peptides produced under low-$[Ca^{2+}]_{free}$ conditions were smaller than those produced at high $[Ca^{2+}]_{free}$ (Figure 3, Tables 1 and 2). At high $[Ca^{2+}]_{free}$, the central portion of the protein was protected, while at low $[Ca^{2+}]_{free}$, the central portion of the protein was more vulnerable to tryptic proteolysis (summarized in Figure 4). These data suggest that the unliganded form of GCAP1 contains a less ordered structure than the liganded form.

Effect of Single EF-Hand Mutations. To inactivate Ca^{2+}-binding loops of GCAP1, the invariant Glu in position 12 (−z) of the EF hand was mutated into Asp (Figure 5). The rationale was to introduce a shorter amino acid that would prevent the coordination of Ca^{2+} ion but preserve the negative charge, thus, minimally affecting the conformation of the

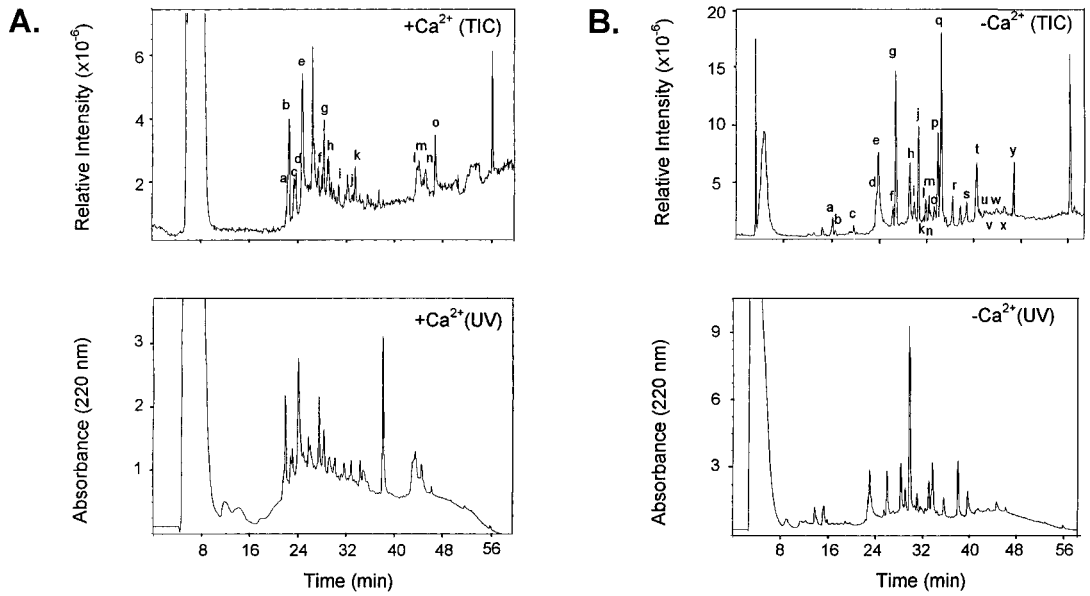

FIGURE 3: Chromatographic profiles of peptides generated during limited proteolysis of GCAP1. LC ESMS was preformed with a PE Sciex API300 triple quadrupole mass spectrometer and UV absorbance monitored at 220 nm. The digests were preformed as described in Materials and Methods. A. Total positive ion current (TIC) and peptide UV map (220 nm) in low $[Ca^{2+}]_{free}$. B. Total positive ion current (TIC) and peptide UV map (220 nm) in high $[Ca^{2+}]_{free}$.

Table 1: Tryptic GCAP1 Peptides Obtained in the Absence of Ca^{2+} Identified by LC ESMS[a]

retention time (min)	obsd mass	residues	calcd mass[b]	error	sequence
16.1 (a)	542.5	179−182	542.4	0.1	R<IVR/R>L
16.5 (b)	891.5	197−205	891.3	0.2	R<ETEAAEADG
18.9 (c)	1489.0	183−196	1488.6	0.4	R<LQNGEQDEEGASGR>E
19.6 (d)	1645.0	182−196	1644.7	0.3	R<R/LQNGEQDEEGASGR>E
23.5 (e)	2363.4	183−205	2363.3	0.1	R<LQNGEQDEEGASGR/ETEAAEADG
23.8 (f)	2519.0	182−205	2519.5	0.5	R<R/LQNGEQDEEGASGR/ETEAAEADG
26.7 (g)	703.8	173−178	703.4	0.4	R<SLDLTR>I
29.1 (h)	1953.0	9−24	1952.9	0.1	K<SVEELSSTECHQWYK
29.9 (i)	1825.0	9−23	1824.8	0.2	K<SVEELSSTECHQWYK>K
30.6 (j)	642.5	94−97	642.3	0.1	R<WYFK>L
31.5 (k)	738.3	41−46	738.4	0.1	R<QFFGLK>N
31.8 (l)	911.8	92−97	911.5	0.3	K<LR/WYFK>L
32.4 (m)	1204.6	163−172	1204.6	0	K<DQMLLDTLTR>S
33.2 (o)	2050.1	24−40	2050.4	0.3	K<K/FMTECPSGQLTLYEFR>Q
33.8 (p)	721.5[c]	41−46	721.4	0.1	R<*QFFGLK>N
33.8 (p)	1921.3	25−40	1920.9	0.4	K<FMTECPSGQLTLYEFR>Q
34.4 (q)	2293.3	98−117	2293.6	0.3	K<LYDVDGNGCIDR/DELLTIIR>A
36.3 (r)	2918.5	94−117	2918.3	0.2	R<WYFK/LYDVDGNGCIDR/DELLTIIR>A
38.7 (s)	3396.7	143−172	3396.8	0.1	K<IDVNGDGELSLEEFMEGVQK/DQMLLDTLTR>S
40.4 (t)	5773.6	121−172	5773.4	0.2	R<AINPCSDSTM...K/DQMLLDTLTR>S
41.8 (u)	5281.3	47−91	5281.0	0.3	K<NLSPWASQYV...LVLK/GK/VEQK>L
42.1 (u)	9841.9	9−91	9842.2	0.3	K<SVEELSSTEC...LVLK/GK/VEQK>L
42.7 (v)	7906.0	25−91	7906.1	0.1	K<FMTECPSGQL...LVLK/GK/VEQK>L
43.8 (w)	2879.6	2−24	2880.0	0.4	Myr-GNIMDGK/SVEELSSTECHQWYK/K>F
45.1 (x)	10768.6	2−91	10768.0	0.6	Myr-GNIMDGK/SV...LVLK/GK/VEQK>L
46.7 (y)	943.8	2−8	943.3	0.5	Myr-GNIMDGK>S

[a] Tryptic peptides from partial digest of GCAP1 (20-min digest), identified by LC ESMS (Figure 3B) are listed by retention time, observed masses, peptide identity, calculated masses, and amino acid sequence. Residue values are based on bovine GCAP1 sequence with N-terminal Met. [b] Peptide calculated mass values are based upon monoisotopic residue weights below 2000 and average residue weights above 2000. Error refers to the difference between the observed and calculated masses. [c] The 721.5 peptide is very likely the pyroglutamate form of 41−46, cyclized during digestion (loss of 17 amu). Symbols (< and >) denote proteolytic cleavage sites.

Ca^{2+}-free form of GCAP1. At low $[Ca^{2+}]_{free}$, the GCAP1-($E^{75}D$) mutant showed a similar dose dependency of GC1 stimulation to native GCAP1 in washed ROS (Figure 6A) and recombinant GC1 (data not shown).[3] At high $[Ca^{2+}]_{free}$, similarly to GCAP1, GCAP1($E^{75}D$) mutant inhibited GC1 basal activity (Figure 6A). GCAP1($E^{111}D$) and GCAP1-($E^{155}D$) mutants had similar dose dependency and GC1 stimulation at low $[Ca^{2+}]_{free}$. However, high $[Ca^{2+}]_{free}$ inactivated these mutants only partially (~50%) (Figure 6A), activities which were not suppressed even at 50 and 500 μM $CaCl_2$ (data not shown). These results suggest that the mutations of the EF-hand loops do not affect stimulation of GC1 at low $[Ca^{2+}]_{free}$ and that the binding of Ca^{2+} to EF2 contributes little to GCAP1 inactivation.

[3] In all studies, both GC in washed ROS and recombinant GC1 expressed in insect cells gave similar results.

Table 2: Tryptic GCAP1 Peptides Obtained in the Presence of Ca^{2+} Identified by LC ESMS[a]

retention time (min)	obsd mass	residues	calcd mass[b]	error	sequence
22.2 (a)	542.3	179−182	542.4	0.1	R<IVR/R>L
22.4 (b)	891.5	197−205	891.3	0.2	R<ETEAAEADG>
23.3 (c)	1489.0	183−196	1488.6	0.4	R<LQNGEQDEEGASGR>E
23.6 (d)	1644.9	182−196	1644.7	0.2	R<R/LQNGEQDEEGASGR>E
24.6 (e)	2363.5	183−205	2363.3	0.2	R<LQNGEQDEEGASGR/ETEAAEADG
24.6 (e)	2519.6	182−205	2519.5	0.1	R<R/LQNGEQDEEGASGR/ETEAAEADG
26.6 (f)	703.5	173−178	703.4	0.1	R<SLDLTR>1
28.2 (g)	1953.0	9−24	1952.9	0.1	K<SVEELSSTECHQWYK/K>F
29.0 (h)	1825.2	9−23	1824.8	0.4	K<SVEELSSTECHQWYK>K
30.7 (i)	738.5	41−46	738.4	0.1	R<QFFGLK>N
32.9 (j)	2050.1	24−40	2050.4	0.1	K<K/FMTECPSGQLTLYEFR>Q
33.4 (k)	721.5*	41−46	721.4	0.1	R<*QFFGLK>N
33.4 (k)	1921.6	25−40	1920.9	0.7	K<FMTECPSGQLTLYEFR>Q
43.8 (l)	22670	9−205	22663.4	6.6	K<SVEELSSTEC...R/ETEAAEADG
43.8 (l)	21794	9−196	21789.6	4.4	K<SVEELSSTEC...EQDEEGASGR>E
44.2 (m)	19796	9−178	19793.5	2.5	K<SVEELSSTEC...TLTR/SLDLTR>I
45.1 (n)	23596	2−205	23589.2	6.8	full length myristoylated protein
46.7 (o)	943.5	2−8	943.3	0.2	Myr-GNIMDGK>S

[a] Tryptic peptides from partial digest of GCAP1 (20-min digest), identified by LC ESMS (Figure 3A)are listed by retention time, observed masses, peptide identity, calculated masses, and amino acid sequence. Residue values are based on bovine GCAP1 sequence with N-terminal Met. [b] Peptide calculated mass values are based upon monoisotopic residue weights below 2000 and average residue weights above 2000. Error referrs to the difference between the observed and calculated masses. [c] The 721.5 peptide is very likely the pyroglutamate form of 41−46, cyclized during digestion (loss of 17 amu). Symbols (< and >) denote proteolytic cleavage sites.

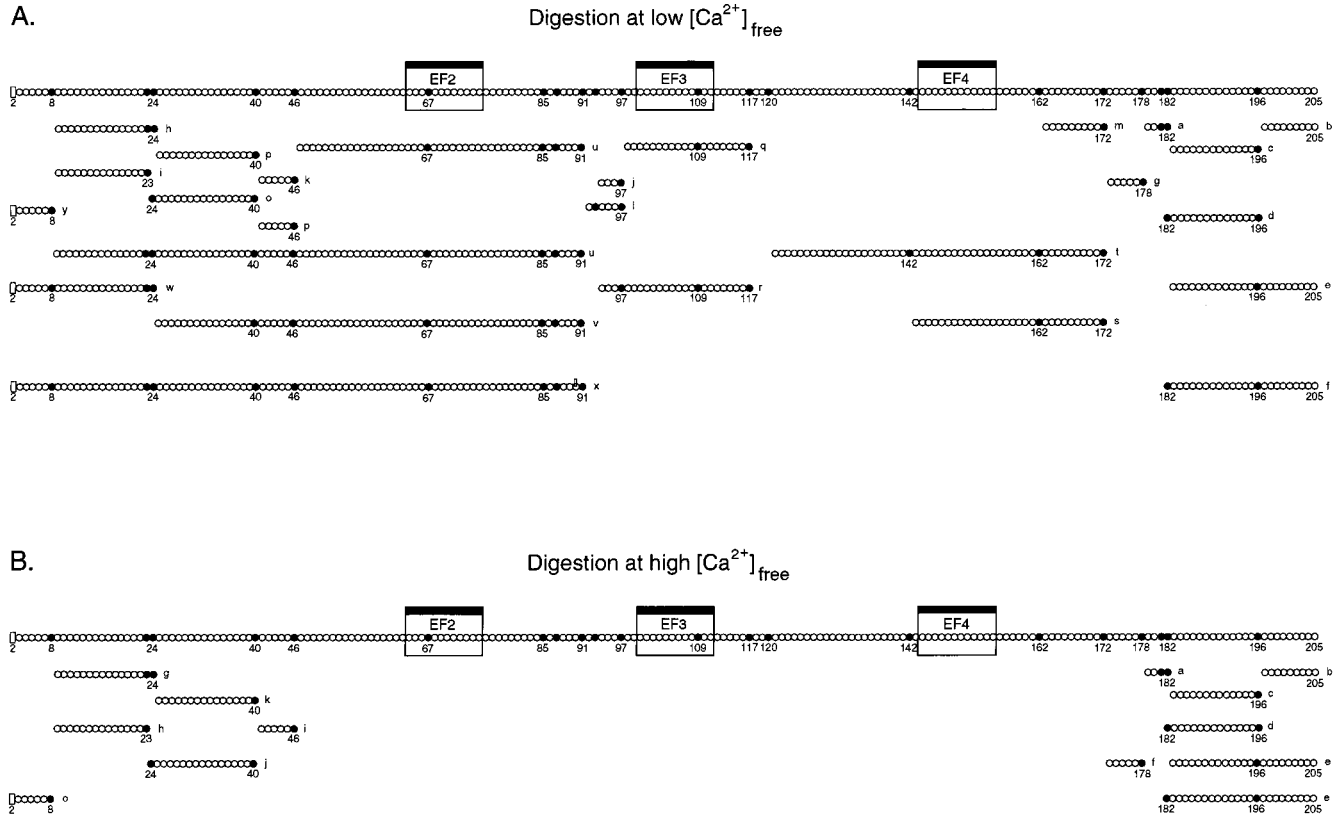

FIGURE 4: Linear structure of GCAP1. Within the linear structure of GCAP1, potential sites of trypsin cleavage (Lys, Arg) are marked as (●). A. In the presence of low $[Ca^{2+}]_{free}$ (40 nM), trypsin cleaves at most of the potential cleavage sites in addition to the N- and C-terminal regions. B. In the presence of high $[Ca^{2+}]_{free}$ (2 μM), trypsin generates N- and C-terminal peptides with the most prominent cleavage sites at K^8 and R^{178}.

Effect of Double and Triple EF-Hand Mutations. The double GCAP1($E^{75}D$,$E^{111}D$) mutant is similar to the single GCAP1($E^{111}D$) and showed a dose dependency of GC1 stimulation similar to native GCAP1 at low $[Ca^{2+}]_{free}$. High $[Ca^{2+}]_{free}$ inactivated this mutant only partially (∼75%) (Figure 6B). However, GCAP1($E^{75}D$,$E^{111}D$) mutant is more susceptible to Ca^{2+} inactivation than GCAP1($E^{111}D$) mutant. The double GCAP1($E^{111}D$,$E^{155}D$) mutant stimulated GC1 maximally at comparable concentrations as native GCAP1, and it was not inactivated at high $[Ca^{2+}]_{free}$ (Figure 6B). As expected, an additional mutation in position $E^{75}D$ did not further affect the properties of GCAP1($E^{111}D$,$E^{155}D$) mutant, although Ca^{2+} could be bound in reduced amounts as determined by the Hummel-Dryer method (*28*). Even nonphysiologically high $[Ca^{2+}]_{free}$ (50 or 500 μM) did not inactivate these mutants (data not shown). GCAP1-

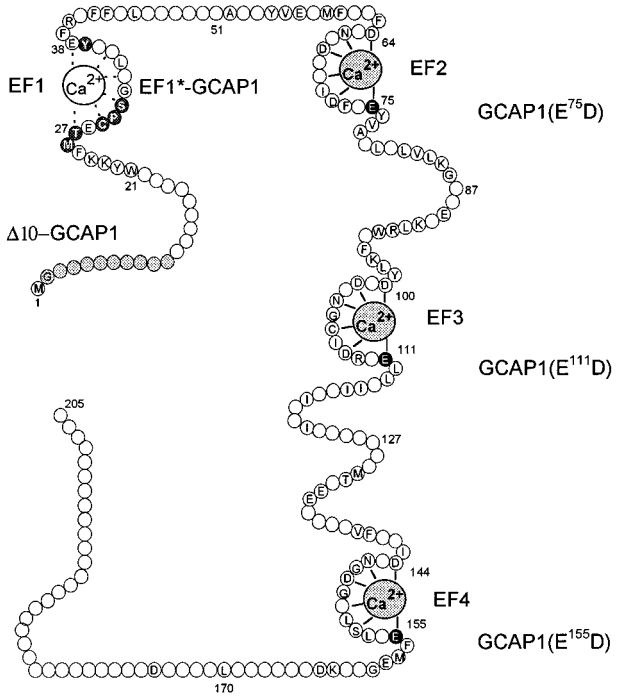

FIGURE 5: Domain structure of GCAP1. The N-terminal Met of GCAP1 is removed and G^2 is N-acylated by fatty acid(s). Conserved residues among bovine, mouse, human, chicken, and frog GCAP1 and GCAP2 are shown throughout the sequence. Δ10-GCAP1 is a deletion mutant (residues marked by different light shading) lacking the N-terminus, respectively. GCAP1 contains three EF-hand motifs (EF2−4) responsible for Ca^{2+} chelation. The EF1-hand motif does not contain residues essential for the Ca^{2+}-binding coordination. To disable the Ca^{2+} binding to EF2-, EF3-, and EF4-hand motifs, invariant Glu residues E^{75}, E^{111}, and E^{155} (residues marked by white letters on black background) were changed to Asp (D). To restore Ca^{2+}-binding properties to the EF1-hand motif, M^{26}, T^{27}, C^{29}, P^{30}, S^{31}, and Y^{37} (residues marked by white letters on shaded background) were substituted by V^{26}, D^{27}, D^{29}, G^{30}, D^{31}, and E^{37} . EF1*-GCAP1 has a functional EF1 motif and nonfunctional EF2−4 motifs.

(E^{75}D,E^{111}D,E^{155}D) mutant did not bind Ca^{2+}, as determined in direct binding assays using gel filtration (Figure 7). Limited proteolysis of this mutant was indistinguishable in low (data not shown) and high [Ca^{2+}] (Figure 7) and similar to the Ca^{2+}-free form of native GCAP1 (Figure 2). These data suggest that the EF3-hand motif (E^{111}D) and EF4-hand motif (E^{155}D mutant) are the most critical and sufficient for Ca^{2+}-sensitive inactivation of GCAP1. Thus, GCAP1-(E^{75}D,E^{111}D,E^{155}D) mutant and GCAP1(E^{111}D,E^{155}D) mutant are constitutively active, and they stimulate GC1 independently of $[Ca^{2+}]_{free}$.

In GCAP1, the EF1-hand motif is disabled for Ca^{2+} binding. To investigate its contribution to GC1 stimulation, we modified its sequence TECPSGQLTLYE to DKDGDGQLTLEE in the triple mutant GCAP1-(E^{75}D,E^{111}D,E^{155}D) (Figure 5). The resulting mutant with a functional EF1 and nonfunctional EF2−4 was shown to bind Ca^{2+} but was inactive in GC1 stimulation (results not shown). These results suggest that residues in the EF1 region are critical in the interaction with GC1 and/or in maintaining the native conformation.

N-Terminal Region of GCAP1 Is Necessary for Inhibition at High $[Ca^{2+}]_{free}$. GCAP1 competed for GC1 with GCAP1-(E^{75}D,E^{111}D,E^{155}D) mutant at high $[Ca^{2+}]_{free}$, with an IC_{50} comparable to the affinity of the constitutively active mutant for GCAP1 (Figure 8A). This is an important observation which suggests that GCAP1 has comparable affinity at high and low $[Ca^{2+}]_{free}$ for GC1, as proposed in our early studies (*2*). Lack of a myristoylated moiety or the N-terminal region of GCAP1 or GCAP2, mutants GCAP1-G2A and Δ10-GCAP1, decreased the inhibition at high $[Ca^{2+}]_{free}$. These truncated mutants did not inhibit GC1 even at 20 μM. Another myristoylated Ca^{2+}-binding protein, recoverin, did not have any effect in this assay.

Competition of GCAP2 with GCAP1 and Additive Stimulation of GC1 with S-100β. Native GCAP2 also competed effectively at high $[Ca^{2+}]_{free}$, with an IC_{50} comparable to the affinity of the constitutively active mutant for GC1 (Figure 8B). This result suggests that GCAP1 and GCAP2 have comparable affinities for GC1. One of several possibilities is that the binding sites for GCAP1 and GCAP2 may at least partially overlap. This conclusion is consistent with the saturable effects of GCAP1 (or GCAP2), and addition of GCAP2 (or GCAP1) does not increase the activity of GC1.[4] Lack of a myristoylated moiety also eliminated inhibition at high $[Ca^{2+}]_{free}$ of GCAP2. Another activator of GC1, S-100β, the physiological role of which is unclear, acted additively with the constitutively active mutant at high $[Ca^{2+}]_{free}$ and relieved inhibition by the Ca^{2+}-occupied native GCAP1 (Figure 8C) or GCAP2, suggesting that GCAP1 (or GCAP2) and S-100β have nonoverlapping binding sites. This experiment also served as an important control, suggesting that if the binding sites are nonoverlapping, then the GC1 stimulation was additive. S-100β did not have any affect of GCAP1-dependent inhibition of the GC1 basal activity at low $[Ca^{2+}]_{free}$.

DISCUSSION

Does GCAP1 Dissociate from GC1 in a Ca^{2+}-Dependent Manner? As a result of this and earlier studies, an interesting mechanism emerges for GC1 stimulation by GCAP1. It appears that GCAP1 forms a stable complex with GC1 and the changes in $[Ca^{2+}]_{free}$ lead to a conformational switch that activates GC1 5−10-fold. These conclusions are based on several lines of evidence including: (a) the presence of GCAP1 in the membrane fraction of ROS independently of [Ca^{2+}] (*2*), (b) competition of Ca^{2+}-loaded GCAP1 with a constitutively active GCAP1 mutant (Figure 8), (c) comparable affinity of Ca^{2+}-loaded and Ca^{2+}-free forms of GCAP1 for GC1 (Figure 1), and (d) cross-linking of GCAP1 with GC1 irrespective of $[Ca^{2+}]_{free}$ (*7*).

GCAP2 dissociates from membranes when it is saturated with Ca^{2+} (*8*); however, this phenomenon is likely to be only observed in the presence of low-ionic strength buffers. In the Ca^{2+}-loaded form, GCAP2 potently competes with the constitutively active mutant form of GCAP1 (Figure 8) or GCAP2 (*8*, *29*), suggesting strong interaction of GCAPs and GC1 at high $[Ca^{2+}]_{free}$. It is worth noting also that both GCAP1 and GCAP2 share topological similarity with calmodulin and recoverin. Ca^{2+} induces conformational changes in these proteins that expose the hydrophobic regions of the

[4] These results are similar to those reported originally by Gorczyca *et al.* (1995). The data were reproduced in the present study using recombinant GCAP1 and GCAP2 at 10-fold higher concentrations of the complementary protein than before, with identical results.

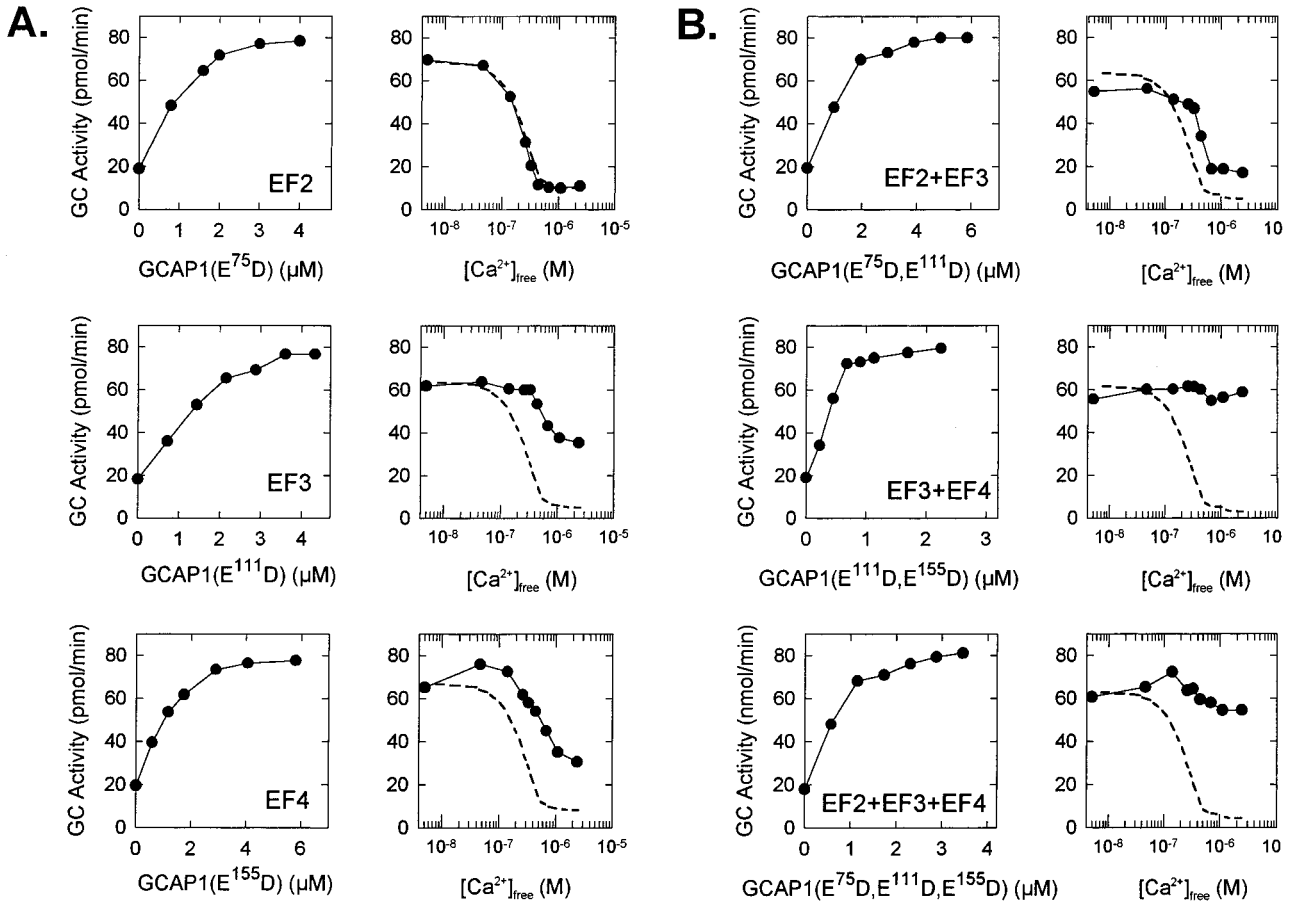

FIGURE 6: Dose dependence and Ca^{2+} titration of GC activity in ROS membranes by GCAP1 mutants. A. Characterization of GC1 stimulation by 2 μM GCAP1 with a mutation of invariant Glu residues to Asp residues that disable Ca^{2+} binding to a single EF-hand motif. B. Characterization of GC1 stimulation by 2 μM GCAP1 with two or three mutations of invariant Glu residues to Asp residues that disable Ca^{2+} binding to two or three EF-hand motifs. The dotted line indicates Ca^{2+} titration for native GCAP1.

molecules and allow strong interactions with some hydrophobic targets.

Do GCAP1 and GCAP2 Interact with GC1 at the Same Binding Site? The binding sites on GC1 for GCAP1 and GCAP2 are at least partially overlapping. These conclusions are derived from the competition of GCAP1 and GCAP2 with the constitutively active GCAP1 mutant (Figure 8). An alternative explanation could be that GCAP2 binding evokes a "dominant" effect on GC1 that could remove the stimulatory effect of GCAP1. This point is illustrated using S-100β protein, another activator of unknown physiological relevance, in the activation of GC1 at high Ca^{2+}. The effect of stimulation by S-100β is additive with the constitutively active GCAP1 mutant, suggesting that the binding sites are independent, but high Ca^{2+}-dependent inhibition by native GCAP1 can be abolished by S-100β, which exerts a "dominant" effect in the stimulation of GC1. GCAP1 and GCAP2 at low $[Ca^{2+}]_{free}$, however, do not stimulate GC1 additively (*2*). Further experiments are needed to bring this important point to a conclusion.

How Do EF-Hand Motifs Regulate the Conformation and Activity of GCAP1? The GCAP1($E^{75}D$) mutant with a disabled EF2-hand motif did not alter the stimulation of GC1, when compared with native GCAP1. The most critical for Ca^{2+}-sensitive inactivation of GCAP1 are the EF3- and EF4-hand motifs, and disabling mutations in these motifs led to partial Ca^{2+} insensitivity. Consistent with these results, the GCAP1($E^{75}D$,$E^{111}D$,$E^{155}D$) and GCAP1($E^{111}D$,$E^{155}D$) mu-

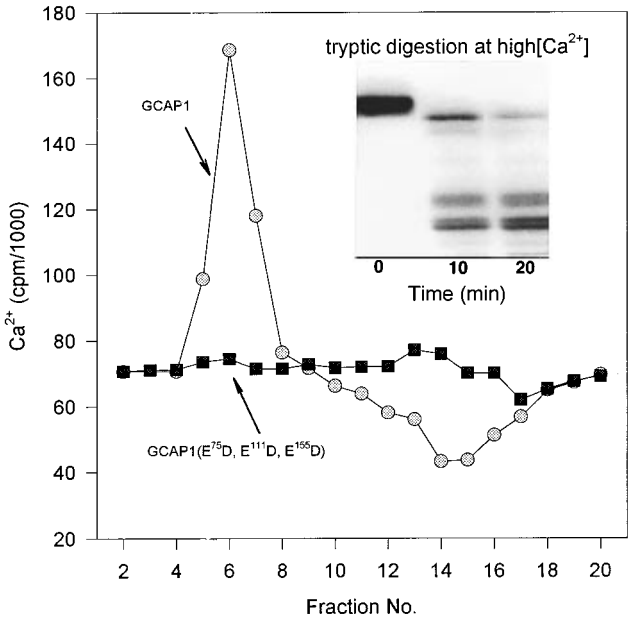

FIGURE 7: Binding of Ca^{2+} to GCAP1 and GCAP1-($E^{75}D$,$E^{111}D$,$E^{155}D$) mutants. Gel filtrations (*28*) of GCAP1 (circles) and its mutants (squares) were carried out using a G-25 Sephadex column (1.6 × 2.5 cm) at a flow rate of 0.2 mL/min. The buffer (10 mM BTP, pH 7.5, 100 mM NaCl) contained 1 μM [^{45}Ca]$CaCl_2$ and 1.6−3.8 μM proteins. *Inset:* Limited proteolysis of GCAP1-($E^{75}D$,$E^{111}D$,$E^{155}D$) mutant by trypsin in the presence of 1 μM $CaCl_2$.

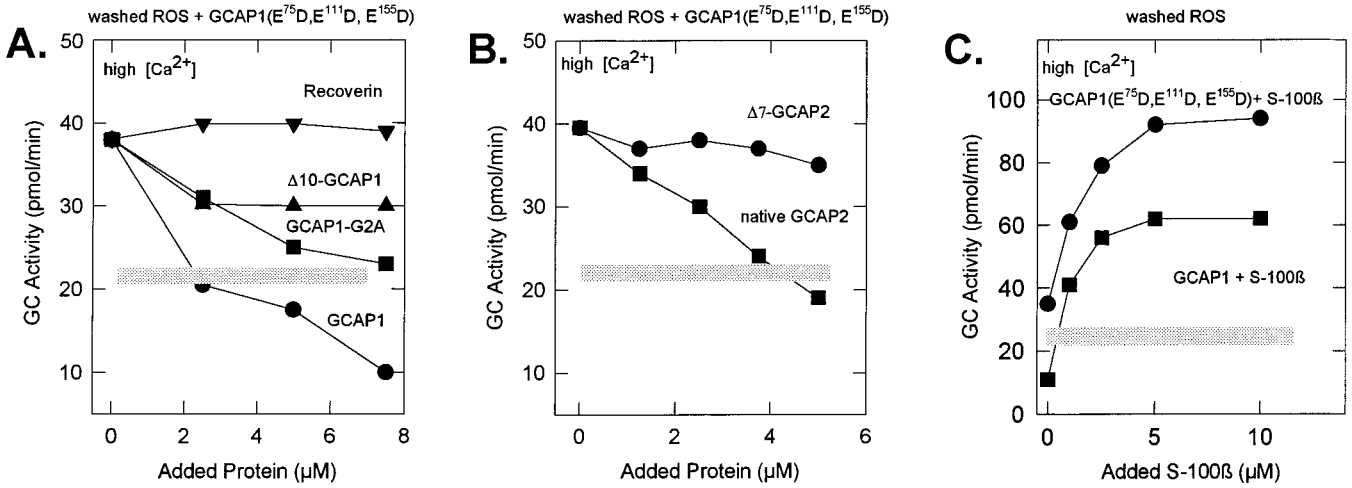

FIGURE 8: Inhibition of GC stimulation by GCAP1 mutants and other Ca^{2+}-binding proteins. A. Inhibition of GC stimulation by GCAP1 mutants. GC in washed ROS devoid of endogenous GCAP1 was stimulated by 1 μM GCAP1($E^{75}D$,$E^{111}D$, $E^{155}D$) mutant at $[Ca^{2+}]_{free} = 10$ μM in the presence of various concentrations of native GCAP1, GCAP1-2A, and Δ10-GCAP1. In control experiments, no inhibition was observed in the presence of recoverin. B. Inhibition of GC stimulation by GCAP1 mutants. GC in washed ROS devoid of endogenous GCAP1 was stimulated by 1 μM GCAP1($E^{75}D$,$E^{111}D$,$E^{155}D$) mutant at $[Ca^{2+}]_{free} = 10$ μM in the presence of various concentrations of native GCAP2 and bacterially expressed GCAP2. **C.** Additive stimulation of GC activity by GCAP1($E^{75}D$,$E^{111}D$,$E^{155}D$) mutant and S-100β. GC in washed ROS devoid of endogenous GCAP1 was stimulated by 1 μM GCAP1($E^{75}D$,$E^{111}D$,$E^{155}D$) mutant and various concentrations of S-100β at $[Ca^{2+}]_{free} = 10$ μM. In control experiments, GCAP1($E^{75}D$,$E^{111}D$,$E^{155}D$) mutant was replaced by GCAP1. Horizontal shaded boxes indicate the range of the basal cyclase activity.

tants are constitutively active, because they stimulate GC1 independently of $[Ca^{2+}]_{free}$. It is worth noting that the sensitivity of GCAP1($E^{75}D$,$E^{111}D$) mutant to Ca^{2+} inactivation is higher than that of the GCAP1($E^{111}D$) mutant. Apparently, the loss of two EF-hand motifs with the EF4-hand motif occupied by Ca^{2+} in GCAP1($E^{75}D$,$E^{111}D$) mutant can lead to a less active conformation than the one assumed by the mutant which lacks only the EF3-hand motif.

Independent from our studies, Dizhoor and Hurley (*29*) investigated the effects of inactivation of GCAP2 by introducing a disabling mutation of invariant Glu to Gln at position 12 of each of the EF-hand motifs individually or in combination. All three EF-hand motifs contributed to the inhibitory properties of GCAP2, and each individual mutant, with an altered EF-hand motif, was fully inactivated by Ca^{2+} (*29*). These data obtained for GCAP1 described in this study differ from those obtained with GCAP2. These functional differences between GCAP1 and GCAP2 could be a result of differences in the primary sequences between these two proteins.

Conformational Changes in GCAP1 upon Ca^{2+} Binding and the Role of the N-Terminal Region. Depletion of Ca^{2+} leads to significant changes in the conformation of GCAP1, generating a structure highly accessible for trypsin. This is surprising, because it is the "unfolded" form of GCAP1 that stimulates with GC1. It is likely that, in the complex, GC1 induces changes in the conformation of unliganded GCAP1 that allow precise coupling between these two proteins. Based on this and earlier studies (*9*), it is apparent that the N-terminal region is necessary for the optimal orientation of GCAP1 in the complex, but it is also apparent that the N-terminal region is indispensable for the high affinity for GC1 and the inhibition of the basal activity of GC1 at high $[Ca^{2+}]_{free}$ (Figure 8). Our data also support the idea that the N-terminus of GCAP2 could produce a similar effect, although sequence similarity of this region is weak.

Is Inhibition of GC1 Basal Activity by the Ca^{2+}-Loaded Form of GCAP1 Physiologically Relevant? Although high-$[Ca^{2+}]_{free}$ inhibition of the *basal activity* of GC1 is a useful tool for studying the interaction between cyclase and GCAPs, it is unclear whether this inhibition is physiologically relevant in photoreceptor cells. The inhibition is observed at $[Ca^{2+}]_{free} > 1$ μM, a concentration which is not likely to be achieved in photoreceptor cells (*30*) with the exception of the immediate vicinity of the cation channel. However, due to localization of both GC1 (*3*) and GCAP1 (*2*) throughout photoreceptor cells, it is conceivable that such regulation is important for processes in cell bodies and synaptic regions of cones and rods. The high-$[Ca^{2+}]_{free}$ inhibition would suppress cGMP production in $[Ca^{2+}]_{free}$-overloaded cells.

ACKNOWLEDGMENT

We thank Dr. Janina Buczylko, Karen A. West, J. Preston Van Hooser, and J. Darin Bronson for help during the course of these studies and also D. Possin for assistance in preparation of figures.

REFERENCES

1. Gorczyca, W. A., Gray-Keller, M. P., Detwiler, P. B., & Palczewski, K. (1994) *Proc. Natl. Acad. Sci. U.S.A. 91*, 4014−4018.
2. Gorczyca, W. A., Polans, A. S., Surgucheva, I. G., Subbaraya, I., Baehr, W., & Palczewski, K. (1995) *J. Biol. Chem. 270*, 22029−22036.
3. Dizhoor, A. M., Lowe, D. G., Olshevskaya, E. V., Laura, R. P., & Hurley, J. B. (1994) *Neuron 12*, 1345−1352.
4. Dizhoor, A. M., Olshevskaya, E. V., Henzel, W. J., Wong, S. C., Stults, J. T., Ankoudinova, I., & Hurley, J. B. (1995) *J. Biol. Chem. 270*, 25200−25206.
5. Polans, A., Baehr, W., & Palczewski, K. (1996) *Trends Neurosci. 19*, 547−554.
6. Shyjan, A. W., de-Sauvage, F. J., Gillett, N. A., Goeddel, D. V., & Lowe, D. G. (1992) *Neuron 9*, 727−737.
7. Duda, T., Goraczniak, R., Surgucheva, I., Rudnicka-Nawrot, M., Gorczyca, W., Palczewski, K., Sitaramayya, A., Baehr, W., & Sharma, R. K. (1996) *Biochemistry 35*, 8478−8482.
8. Olshevskaya, E. V., Hughes, R. E., Hurley, J. B., & Dizhoor, A. M. (1997) *J. Biol. Chem. 272*, 14327−14233.

9. Otto-Bruc, A., Buczylko, J., Surgucheva, I., Subbaraya, I., Rudnicka-Nawrot, M., Crabb, J. W., Arendt, A., Hargrave, P. A., Baehr, W., & Palczewski, K. (1997) *Biochemistry 36*, 4295−4302.
10. Koutalos, Y., & Yau, K.-W. (1996) *Trends Neurosci. 19*, 73−81.
11. Perrault, I., Rozet, J. M., Calvas, P., Gerber, S., Camuzat, A., Dollfus, H., Chatelin, S., Souied, E., Ghazi, I., Leowski, C., Bonnemaison, M., LePaslier, D., Frezal, J., Dufier, J. L., Pittler, S., Munnich, A., & Kaplan, J. (1996) *Nature Genet. 14*, 461−464.
12. Semple-Rowland, S. L., Gorczyca, W. A., Buczylko, J., Helekar, B. S., Ruiz, C. C., Subbaraya, I., Palczewski, K., & Baehr, W. (1996) *FEBS Lett. 385*, 47−52.
13. Semple-Rowland, S. L., Evans, J., Bronson, D., Ludwig, E., Buczylko, J., Palczewski, K., & Baehr, W. (1997) *Invest. Ophthalmol. Visual Sci. 38*, S910.
14. Lowe, D. G., Dizhoor, A. M., Liu, K., Gu, Q., Spencer, M., Laura, R., Lu, L., & Hurley, J. B. (1995) *Proc. Natl. Acad. Sci. U.S.A. 92*, 5535−5539.
15. Garbers, D. L., & Lowe, D. G. (1994) *J. Biol. Chem. 269*, 30741−30744.
16. Liu, X., Seno, K., Nishizawa, Y., Hayashi, F., Yamazaki, A., Matsumoto, H., Wakabayashi, T., & Usukura, J. (1994) *Exp. Eye Res. 59*, 761−768.
17. Pozdnyakov, N., Yoshida, A., Cooper, N. G., Margulis, A., Duda, T., Sharma, R. K., & Sitaramayya, A. (1995) *Biochemistry 34*, 14279−14283.
18. Bradford, M. M. (1976) *Anal. Biochem. 72*, 248−254.
19. Laemmli, U. K. (1970) *Nature 227*, 680−685.
20. Maundrell, K. (1993) *Gene 12*, 127−130.
21. Okazaki, K., Okazaki, N., Kume, K., Jinno, S., Tanaka, K., & Okayama, H. (1990) *Nucleic Acids Res. 18*, 6485−6489.
22. Palczewski, K., Subbaraya, I., Gorczyca, W. A., Helekar, B. S., Ruiz, C. C., Ohguro, H., Huang, J., Zhao, X., Crabb, J. W., Johnson, R. S., Walsh, K. A., Gray-Keller, M. P., Detwiler, P. B., & Baehr, W. (1994) *Neuron 13*, 395−404.
23. Smith, A. M., & Klugman, K. P. (1997) *Biotechniques 22*, 438−442.
24. Surguchov, A., Bronson, J. D., Banerjee, P., Knowles, J. A., Ruiz, C., Subbaraya, I., Palczewski, K., & Baehr, W. (1997) *Genomics 39*, 312−322.
25. Otto-Bruc, A., Fariss, R. N., Haeseleer, F., Huang, J., Buczylko, J., Surgucheva, I., Baehr, W., Milam, A. H., & Palczewski, K. (1997) *Proc. Natl. Acad. Sci. U.S.A. 94*, 4727−4732.
26. Kapron, J. T., Hilliard, G., Lakins, J., Tenniswood, M., West, K. A., Carr, S. A., & Crabb, J. W. (1997) *Protein Sci. 6*, 1−14.
27. Papermaster, D. S. (1982) *Methods Enzymol. 81*, 48−52.
28. Hummel, J. P., & Dryer, W. J. (1962) *Biochim. Biophys. Acta 63*, 531−532.
29. Dizhoor, A. M., & Hurley, J. B. (1996) *J. Biol. Chem. 271*, 19346−19350
30. Gray-Keller, M. P., & Detwiler, P. B. (1994) *Neuron 13*, 849−861.
31. Dizhoor, A. M., Chen, C. K., Olshevskaya, E., Sinelnikova, V. V., Phillipov, P., & Hurley, J. B. (1993) *Science 259*, 829−832.

BI972306X